

Validation of a pXO2-A PCR Assay To Explore Diversity among Italian Isolates of *Bacillus anthracis* Strains Closely Related to the Live, Attenuated Carbosap Vaccine

M. Muscillo,^{1*} G. La Rosa,¹ M. Sali,¹ E. De Carolis,¹ R. Adone,² F. Ciuchini,²
and A. Fasanella³

Department of Environment and Primary Prevention¹ and Department of Food and Veterinary Medicine,²
Istituto Superiore Sanità Roma, Rome, Italy, and Department of Anthrax Reference Institute
of Italy at Istituto Zooprofilattico Sperimentale di Puglia e Basilicata, Foggia, Italy³

Received 10 February 2004/Returned for modification 21 September 2004/Accepted 4 May 2005

Several circulating *Bacillus anthracis* strains isolated in Italy and belonging to the A1.a cluster, genotype 3 (A1.a-3) are genotypically indistinguishable from Carbosap, a live attenuated vaccine strain, containing both pXO1 and pXO2 plasmids. The genotype was assessed by using eight-locus multilocus variable-number tandem repeat analysis. We describe here the use of a ninth locus able to explore variability among strains that have the same genotype. It is important to be able to genotype the wild isolate of *B. anthracis* strains from outbreaks of anthrax in areas where Carbosap vaccination of cattle and sheep is common practice. A total of 27 representative field strains isolated in Italy and four vaccinal strains, namely, Carbosap, Sterne, Pasteur I, and Pasteur II, were characterized by a ninth marker, called pXO2-A. Twenty-three field strains were genotype 3 and therefore identical to Carbosap. The marker was in the pXO2 plasmid and is based on the polymorphism of the already-known VX2-3 locus. Detection was obtained by PCR with fluorescence-labeled forward primers in order to produce appropriate fragments for capillary electrophoresis with an ABI 310 genetic analyzer. Genetic relationships showed heterogeneity in all of the examined samples. Interestingly, with respect to genotype 3, samples grouped into eight different subtypes, A to H, and the subtype G, had only two samples indistinguishable from Carbosap. The results of the present study confirm the validity of a hierarchical progressive protocol for discrimination among closely related isolates.

The recent wave of bioterrorism (3, 4, 9, 10) has caused several billion dollars of losses to the global economy. Efforts to prevent future terrorist attacks in the United States (2) led to the availability of the whole genome of *Bacillus anthracis* strains isolated in Florida, New York, and Washington, D.C. On The Institute for Genomic Research (TIGR) website (www.tigr.org) there are both finished (19) and unfinished genome projects of several anthrax strains as part of an effort to create a database of species variation.

When comparison of complete genome sequences was still not possible, numerous studies demonstrated the lack of molecular polymorphism within *B. anthracis* (12). Later, sequencing projects accelerated improvement in molecular typing of these pathogens. An eight-locus multilocus variable-number tandem repeat (VNTR) analysis (8-MLVA) has become the gold standard for the assessment of genetic relationships within the representative worldwide clones (13). The 8-MLVA approach provided a multiple-factor genetic analysis with six chromosomal, one pXO1 locus, and one pXO2 locus markers, with a discriminatory power of 42 alleles. A comparative genome sequencing for discovery of novel polymorphisms in *B. anthracis* (20) provided a powerful new tool for investigating infectious disease outbreaks. A total of 64 new polymorphic sites, including single-nucleotide polymorphism, VNTR, sin-

gle-nucleotide repeats, and insertions, were reported. A recent approach (14) showed the usefulness of a nested hierarchical approach, applicable to a wide range of pathogens, that uses a progression of diagnostic genomic low-resolution loci and, ultimately, high-resolution loci.

For safety reasons and ease of handling in the laboratory, many investigators have used attenuated vaccine strains carrying one of the two plasmids in studies of toxin and capsule gene expression. The widely studied Sterne (pXO1⁺/pXO2⁻) is nonencapsulated and toxigenic, whereas Pasteur I type (pXO1⁻/pXO2⁺) is encapsulated and nontoxigenic. However, atypical Pasteur vaccine strains isolated previously (21) showed the pXO1⁺/pXO2⁺ profile, and one of them, the Pasteur II strain, was recently used in real-time PCR studies of *pag* and *cap* genes (15). Reference data report that two of three *B. anthracis* vaccine strains formerly used as antianthrax vaccine strains for cattle in Argentina showed the two-plasmid pattern (5). In Italy an atypical *B. anthracis* vaccine strain, Carbosap (pXO1⁺/pXO2⁺), has been used since 1949 for immunization of cattle and sheep. Although it carries both plasmids, it shows virulence in guinea pigs and mice and is not pathogenic for rabbits (1, 7).

In order to evaluate the mechanism of attenuation in the *B. anthracis* vaccine strain Carbosap, a previous study (1) sequenced the structural genes encoding for the major virulence factors (*cya*, *lef*, and *pagA*), two *trans*-acting regulatory genes (*atxA* and *pagR*), and the *gerX* operon involved with germination within macrophages. No molecular differences were found

* Corresponding author. Mailing address: Dipartimento Ambiente e Connessa Prevenzione Primaria, Istituto Superiore di Sanità, Viale Regina Elena 299, 00161 Rome, Italy. Phone: 39 06 49902718. Fax: 39 06 49902718. E-mail: muscillo@iss.it.

TABLE 1. Gold standard 8-MLVA^a

ID of fluorescence PCR ^b	Locus	ID primer	Sequence (5' to 3') ^c
31	<i>vrrA</i>	538-fam-f 93-r	CAC AAC TAC CAC CGA TGG CAC A GCG CGT TTC GTT TGA TTC ATA C
32	<i>vrrB1</i>	539-fam-f 95-r	ATA GGT GGT TTT CCG CAA GTT ATT C GAT GAG TTT GAT AAA GAA TAG CCT GTG
33	<i>vrrB2</i>	540-fam-f 184-R	CAC AGG CTA TTC TTT ATC AAA CTC ATC CCC AAG GTG AAG ATT GTT GTT GA
34	<i>vrrC1</i>	185-f 541-fam-r	GAA GCA AGA AAG TGA TGT AGT GGA C CAT TTC CTC AAG TGC TAC AGG TTC
35	<i>vrrC2</i>	542-hex-f 188-r	CCA GAA GAA GTG GAA CCT GTA GCA C GTC TTT CCA TTA ATC GCG CTC TAT C
97	CG3	543-tet-f ^d 190-r	TGT CGT TTT ACT TCT CTC TCC AAT AC AGT CTA TGT TCT GTA TAA AGG GCA T
98	PXO1-aat	544-fam-f 392-r	CAA TTT ATT AAC GAT CAG ATT AAG TTC A TCT AGA ATT AGT TGC TTC ATA ATG GC
102	PXO2-at	545-hex-f 193-r	TCA TCC TCT TTT AAG TCT TGG GT GTG TGA TGA ACT CCG ACG ACA

^a When indicated, primers were 5' labeled with fam, hex, or tet. Each fluorescent dye has an excitation wavelength of 488 nm and an emission wavelength of 518, 556, or 538 nm. The rox-labeled standard has an excitation wavelength of 575 nm and an emission wavelength of 602 nm. Abbreviations: f, forward, r, reverse.

^b ID, identification number.

^c According to Keim et al. (13).

^d This primer was ned labeled in the original study.

compared to a *B. anthracis* virulent strain. An approach using real-time PCR for the *lef* gene (17) led to similar results.

It is important to be able to use advanced methods to distinguish *B. anthracis* strains isolated from anthrax outbreaks in areas where Carbosap vaccination is common practice. As far as the PCR test to assess the virulence of *B. anthracis* is concerned, the Organization International Épizooties (OIE) (18) suggests using biomolecular tests which, however, are not able to distinguish wild strains from vaccines with the Carbosap plasmidic profile pXO1⁺/pXO2⁺.

The main aim of the present study was to reinforce the gold standard 8-MLVA protocol by adding another locus selected with the help of computational analyses of the numerous polymorphic loci recently discovered in *B. anthracis*.

Carbosap, some representative wild Italian *B. anthracis* strains and other reference strains, such as Pasteur I, Pasteur II, and Sterne strain, were included in the present study.

MATERIALS AND METHODS

***B. anthracis* isolates and DNA extraction and purification.** The present study is based on 27 wild *B. anthracis*, three vaccinal strains including Pasteur I (ATCC 4229, B. Virat, Institut Pasteur, strain 75.16, 1975) for which a pXO1⁻/pXO2⁺ pattern was reported on the original enclosed sheet, Pasteur II (B. Virat, Institut Pasteur, strain 74.12, 1974) without any direct indications of the plasmidic profiles, the pXO1⁺/pXO2⁻ Sterne used in vaccine production (B. Virat, Institut Pasteur, strain 77.2, VCSA 1947), and the Italian attenuated vaccine Carbosap. All of the wild *B. anthracis* strains used here were isolated in outbreaks involving unvaccinated cattle, sheep, and goats living in different geographic areas. Samples and genetic classification were obtained from the Department of Anthrax Reference Institute of Italy at the Istituto Zooprofilattico Sperimentale di Puglia e Basilicata, Foggia, Italy. All of the available genotype 3 strains were used. Two pairs of samples, one of genotype 12 and another of genotype 1, were included in the present study in order to have an idea of the extension, if any, of the

pXO2-A polymorphism to other genotypes. All bacterial strains were grown in 250 ml of tryptone soy broth with shaking at 37°C per 16 h. Cultures were washed three times in sterile phosphate-buffered saline (pH 7.3). The pellet was suspended in 5 ml of sterile deionized water and then transferred to 25-ml Corex glass screw-top tubes. The bacterial suspension was boiled for 20 min. It then was centrifuged at 4,100 rpm for 45 min. The supernatant was collected and stored in 2-ml sterile tubes at -20°C.

Standard 8-MLVA analysis. All samples were genotyped according to the gold standard 8-MLVA (13) with slight modifications (Table 1). Forward primer CG3 was tet labeled instead of ned labeled because the latter was not available from our provider (Primm, Milan, Italy). Typically, 10-μl portions of the PCR products were electrophoretically analyzed on ethidium bromide-agarose gels in order to test the success of the reaction. The remaining 40 μl was used for sequencing and for fragment analysis. All PCRs were performed with Platinum Taq (Invitrogen Corp.) under the same assay conditions as in the original method and using a GeneAmp PCR System 9700 (Applied Biosystems, Foster City, CA) that is certified annually by the European Repair Centre (Applera Europe BV, Nieuwerkerk aan den IJssel, The Netherlands), according to the standards of the Dutch Council for Accreditation (NKO).

For the reader's convenience, primers and PCRs are shown in Table 1. The reported identifications are the codes of a PostgreSQL database, which keeps track of all primers and PCR.

In silico computational analysis of the known polymorphic loci. All of the available finished or unfinished (contigs) *B. anthracis* strain sequences were downloaded from GenBank and from the TIGR website. In addition to the *B. anthracis* prototype, the following genomes were included: Ames Ancestor 0581, Ames Florida A2012, A0039, A1055, Australia-94, CNEVA-9066, France, Kruger-B, Vollum, and Western North America USA6153. One of the four Florida files was released by TIGR after a direct request from one of the authors and was particularly useful. It consisted of a set of 1,000-bp regions centered on each reported polymorphism in order to allow investigators to identify and test these markers on any other anthrax strain.

All of the sequences were scanned using the FINDPATTERNS program of the Wisconsin GCG package (Accelrys, Ltd., Cambridge, United Kingdom) with a complete panel of pattern data (data not shown) for each known polymorphic site. The pattern-data for VX2-3 was "CCGACCT(A){5;}CATACTACC." The brackets indicate some constraints according to a general Unix code: {5;} from

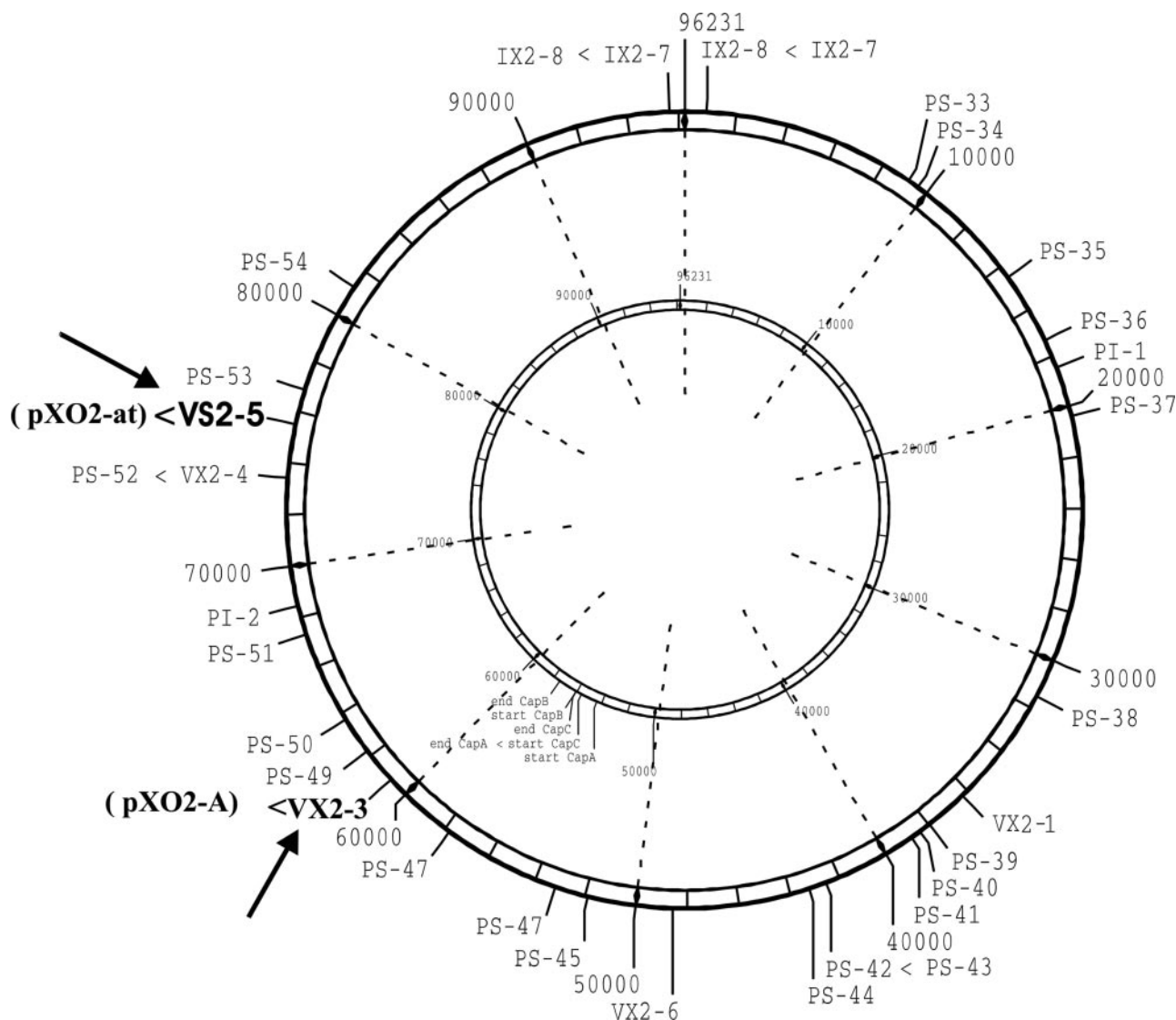


FIG. 1. *B. anthracis* map of the pXO2 (af188935) plasmid polymorphic loci. The origin and end (96231) of the plasmid are shown on the outer circle. The arrows show the two loci of pXO2 plasmid analyzed here. The corresponding PCR alias names are reported in brackets. All of the potential polymorphic loci are mapped with FINDPATTERN as described in Materials and Methods. The loci name are reported unabridged as indicated in a previous article (19). For convenience, the locations of the known virulent genes are mapped in the inner circle. Abbreviations: VX, variable number tandem repeats; IX, insertions; PS, single nucleotide polymorphism; pXO2, plasmid pXO2; -at, tandem repeats of dinucleotides AT; -A, single A repeats.

a minimum of "5" (A) to ∞ . Flanking sequences were constraints able to identify exactly the VX2-3 locus in all of the examined sequences. The MAPSORT and MAPLOT programs of the GCG package were used to reconstruct the map of polymorphic loci. This procedure allowed us to map the pXO2 plasmid with the known polymorphic loci (Fig. 1).

The ninth locus located on pXO2 plasmid: the pXO2-A PCR test. The primer sequences for carrying out the pXO2-A test are reported in Table 2. Primers were engineered in order to include the VX2-3 poly(A) region (20). Nucleotide positions and predicted base pair lengths of PCR products referred to the *B. anthracis* pXO2 plasmid (accession number AFG188935).

These primers were designed to provide uniquely sized fluorescent (PCRs 24, 27, 28, and 29) amplicons (Table 2). In order to increase the sensitivity and specificity of the test at molecular level, several sets of PCR tests were designed. First, an adequate aliquot of the original DNA sample was mixed with all of the necessary PCR reagents, 22 pmol of each primer (406-f/407-r), in a final volume of 100 μ l (PCR 24, Table 2). A 506-bp amplicon was obtained in this step. In the second PCR round, 1 μ l of this mixture was amplified using the primers 462-f_{fam}/420-r (PCR 28, Table 2). The 463-f_{hex}/420-r (Carbosap_{hex}, PCR 29) PCR

was set up in parallel for Carbosap in order to get a Carbosap_{hex}-labeled fragment to use as a dedicated 323-bp fluorescent size marker in all of the runs. As a rule, because the starting sample was available with high DNA content, PCR 24 was bypassed carrying out the PCR 28 as non-nested, simply by using directly 5 μ l of the crude DNA sample. In the nested protocol, PCR 28, was performed by mixing, in a final volume of 50 μ l: 5 μ l of *Taq* buffer (10 \times), 1 μ l of deoxynucleoside triphosphates (10 mmol liter⁻¹), 22 pmol of primers 462-f_{fam} and 420-r, 0.04 U of Platinum *Taq* polymerase (Life Technologies/Gibco-BRL, Gaithersburg, MD)/ μ l, and 1 μ l of DNA of PCR 24 mixture. The PCR thermocycling conditions were as follows: incubation at 95°C for 5 min to activate the DNA polymerase, followed by 35 cycles at 95°C for 20 s, 55°C for 30 s, and 72°C for 2 min., with a final step of 10 min at 68°C. In most cases, 10 μ l of the PCR products was analyzed on ethidium bromide-agarose gels as described above. This step was not mandatory but was used to test the success of the reaction. The remaining 40 μ l was used directly for fragment analyses, without DNA purification.

Automated genotype analysis. Fragment analysis in denaturing conditions was carried out by using the capillary automatic sequencer ABI PRISM 310 Genetic Analyzer (Applied Biosystems). As a size marker, the PRISM GeneScan-500

TABLE 2. Primers used for pXO2-A locus test of the VX2-3 locus shown in the plasmid map^a

PCR no.	Primer	Sequence (5' to 3')	5' position ^b	Predicted length (bp) for <i>B. anthracis</i>
24	406-f	+CAC GAA AGT TTA AAT TGT ACC GCA GA	60590	506
	407-r	-AGA GTT ATT GGA AAA CCA GGA GAT AC	61095	
27	462-fam-f	+TCA ACT TAA GTA AAT TCT CCT TTT CCA	60663	232 (fam)
	464-r	-CCC ATC GAA CGT GTT CTA GCT ACA GTA	60894	
28	462-fam-f	TCA ACT TAA GTA AAT TCT CCT TTT CCA	60663	330 (fam)
	420-r	-CTG CTA TGG ATC AAA AAT GGA TAG TA	60992	
29	463-hex-f	+TCA ACT TAA GTA AAT TCT CCT TTT CCA	60663	330 (hex)
	420-r	-CCC ATC GAA CGT GTT CTA GCT ACA GTA	60894	

^a Plasmid map shown in Fig. 1.

^b Nucleotide positions refer to *B. anthracis* (accession number AF188935).

ROX (usually called ROX500; Applied Biosystems) was used. This standard is a mixture of a carboxy rhodamine-labeled fragments ranging from 35 to 500 bp, which are generally displayed as red peaks (Fig. 2).

The PCR products were run, without purification, in order to genotype samples in a progressive hierarchical way (8 + 1). For a profile of all of the eight loci, 2.0 µl of each PCR product (PCRs 31 to 35, 97, 98, and 102), 24 µl of formamide, 2.0 µl of Carbosap_{-hex} marker (PCR 29), and 3 µl of ROX500 were mixed, denatured at 95°C for 5 min, and then analyzed. For the ninth locus (Fig. 2), 2.5 µl of the PCR product 28, 24 µl of formamide, 2.5 µl of Carbosap_{-hex} marker (PCR 29), and 0.5 µl of ROX500 were mixed and then denatured as previously described.

The separation of fragments was carried out at 15,000 V at 50°C in a 47-cm-by-50-µm capillary filled with POP4 matrix.

Data analysis. Genescan and genotype software packages (Applied Biosystems) were used to quickly analyze the electropherograms. The computing of molecular size of VNTR loci was usually performed with Genotyper software analysis in a complete automatic style. This method was unfortunately not able to intercept the *vrnC1* and *vrnC2* values, which were out of the ROX500 range; they were therefore calculated by sequencing. Because the apparent electrophoretic sizes of the DNA fragments were not always exactly the same as the size determined by DNA sequencing, these two and the other six loci were adjusted according to the standard genotypes selected from the references (13). No reference data were available for the 9th locus, so it has been reported as determined experimentally by fragment analysis. As shown in Table 3, using the values of all of the runs (column 7), a mean value of Carbosap_{-hex} internal standard was computed, and therefore the sample data (column 4) were normalized (column 5) by using a correction factor (column 8).

The graphic representation of genetic profiles is reported in Fig. 3. For this purpose, a very suitable and freely downloadable program (11) is the START (sequence type analysis and recombinational tests) program, which can import and export data in spreadsheet format and is able to handle base pair fragments as well as sequences. The latest version of this software can be downloaded (<http://outbreak.ceid.ox.ac.uk/software.htm>).

RESULTS

The recently reported polymorphic loci of *B. anthracis* strains (20) and comparison among TIGR available sequences were helpful in reconstructing the complete map of discriminatory markers present in pXO2 plasmids (Fig. 1). The polymorphic loci in pXO2 are scattered throughout the genome and, more interestingly, the mapping work predicted that the VX2-3 locus would be the highest discriminatory marker, showing extreme variability among the available TIGR sequences. Single "A" repetitions were 36 (Ames Ancestor 0581), 35 (Ames Florida A2012), 24 (*B. anthracis*), 20 (A1055 and Vollum), 14 (Western North America USA6153), 12 (A0039 and Australia 94), 9 (CNEVA-9066 and France), and 8 (Kruiger B). The poly(A) stretch maps downstream the end of

the *capB* region of the plasmid and predicted several new alleles (at least 28). Tables 1 and 2 report all primers and PCR combinations used in this study. The ID code reported for all of them turned out to be a reliable strategy for referencing unambiguously all of the steps of the protocols described here.

The improved 9-MLVA had the new locus located within the 300- and 340-bp peaks of the ROX500 standard (Fig. 2). Numerical results for all of the loci are reported in Fig. 3, displayed along with the isolate codes. Genotyper software showed a good linearity of size markers, which were well distributed and predicted an accurate estimation of pXO2-A fragment size. As shown in Table 3, the mean value of the Carbosap pXO2-A fragment was 323.11 bp with a standard deviation, calculated on 30 different independent runs, of 0.34 bp. All of the values were approximate after normalization (Table 3, column 5). The results were confirmed in duplicate experiments.

Eight subtypes were observed for genotype 3, two were observed for genotype 1, and two were observed for genotype 12. Subtypes of genotype 3 were tentatively named, for convenience, A-H (column 6, Table 3). These subtypes corresponded to fragments ranging from 317 to 325 bp. Carbosap and two samples (samples 458 and 457) were grouped into subtype G. For convenience, Pasteur I, even if it has an incomplete pattern and cannot be genotyped like the other samples, was included in the G group. All of the genotype 3 samples were different from Carbosap and were subtyped in seven groups (A, B, C, D, E, F, and H). The genotype 1 (samples 419 and 420) and genotype 12 samples (samples 421 and 425) also showed heterogeneity, confirming the usefulness of the pXO2-A test in hierarchically subtyping strains.

Representative electropherograms from 8 independent runs of genotype 3 are reported in Fig. 2. The Carbosap_{-hex} (sample 424) internal standard and samples_{-fam} (samples 472 [A], 466 [B], 460 [C], 462 [D], 464 [E], 422 [F], 457 [G], and 427 [H]) are shown in different colors. The ROX500 profile (red peaks) is also reported for convenience. As shown in group F of Fig. 2, differences of 1 bp between sample 22 and Carbosap sample 424 were well shown in our experimental conditions. Differences of more than 1 bp, as shown in group A, gave very distinct peaks. Two wild samples, 457 and 458, and Pasteur I (pXO1⁻/pXO2⁺) have the 323 allele of Carbosap. As shown in group G of Fig. 2, the representative *B. anthracis*, strain 10

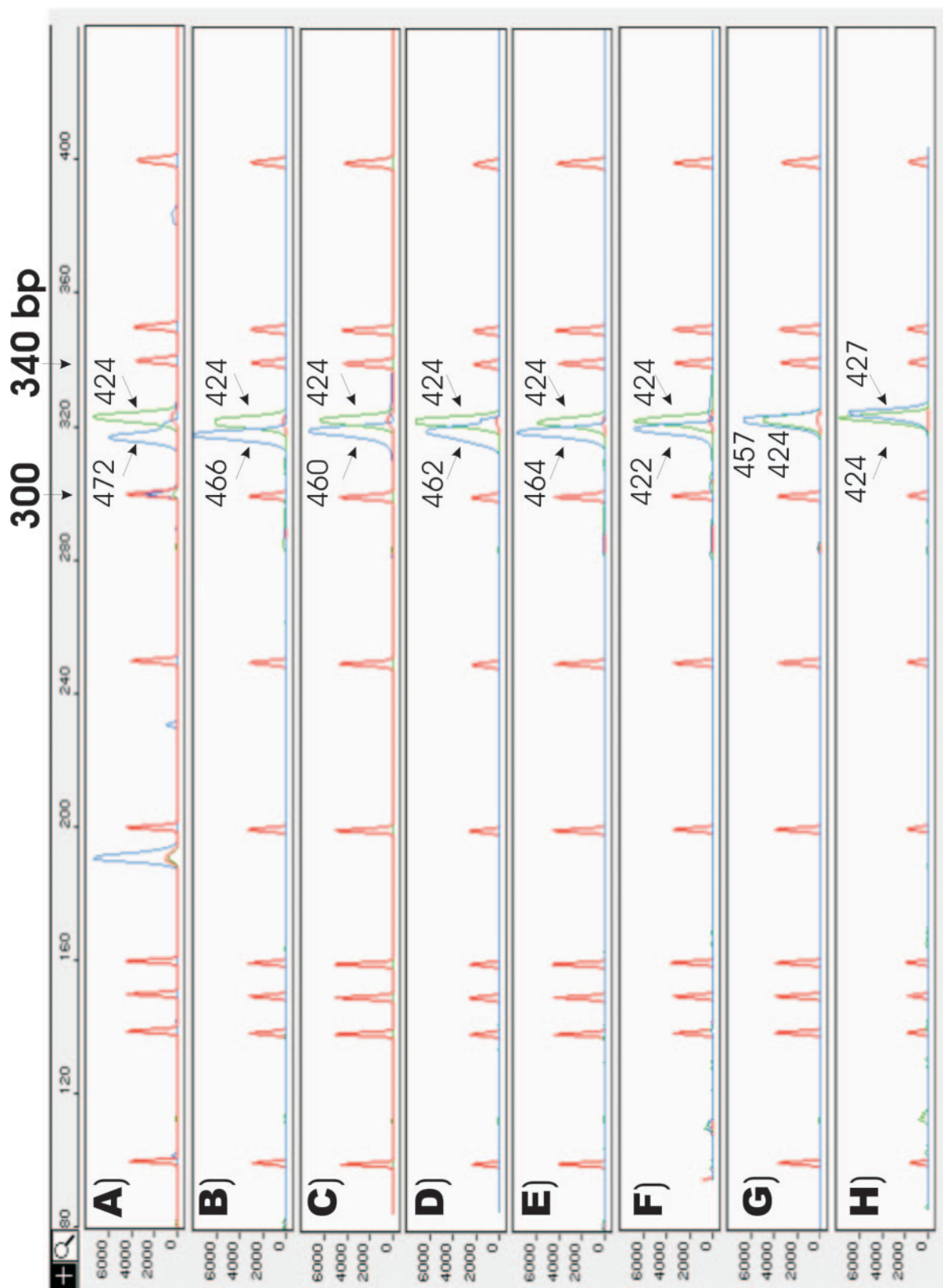


FIG. 2. *B. anthracis* genotype 3 polymorphisms. This figure reports a combined screen capture image of capillary fluorescent electrophoresis of the pXO₂-A test. Colors of samples (blue), Carbosap (green), and ROX500 (red) correspond to different fluorescent labels. The Carbosap_{hex} and Carbosap_{fam} runs are not reported here because peaks perfectly overlapped, similarly to those shown in panel G. All of the graphs were compared after normalization of the profiles with the genotype program according to the internal standard. The heights of the peaks were adjusted to the same range of absorbance, as shown on the left side of each picture. The keys shown in the figure are those reported in Table 3, i.e., sample 424 Carbosap, sample 472, *B. anthracis* strain 10 and so on. On the top of the figure, the 300- and 340-bp marker sizes of ROX500 are shown. From panels A to H the computed peak shift "sample/Carbosap" values were -5, -4, -3, -2, -1, 0, and +1 bp, respectively.

TABLE 3. Genotyping results of pXO2-A test^a

Local ID	<i>B. anthracis</i> strain	Genotype	Length (bp) of sample peak determined by Gene Scan (SP)	Normalized peak against the mean value (SP × R)	Subtype	Carbosap value determined in each run (CP) ^b	Correction factor (R = MV/CP)
461	28	3	317.28	317	A	323.50	0.99881
467	51	3	317.13	317	A	322.75	1.00113
472	66	3	316.83	317	A	323.29	0.99946
473	67	3	317.59	317	A	323.72	0.99813
544	Pac	3	316.65	317	A	322.68	1.00135
466	48	3	318.11	318	B	323.10	1.00005
471	62	3	317.77	318	B	322.76	1.00110
460	27	3	319.65	319	C	323.30	0.99943
543	Cap	3	319.70	320	D	322.81	1.00094
463	36	3	320.18	320	D	323.36	0.99924
545	285	3	319.69	320	D	322.72	1.00122
469	59	3	319.43	320	D	322.88	1.00073
462	33	3	320.20	320	D	323.41	0.99909
470	61	3	320.02	320	D	323.43	0.99903
456	5	3	321.10	321	E	323.24	0.99961
459	17	3	321.15	321	E	323.68	0.99825
464	39	3	320.46	321	E	322.71	1.00125
468	52	3	320.71	321	E	322.75	1.00113
546	7202	3	320.46	321	E	322.71	1.00125
422	Gent	3	321.29	322	F	322.73	1.00119
465	43	3	322.56	322	F	323.29	0.99946
457	10	3	322.96	323	G	322.96	1.00048
458	12	3	323.48	323	G	323.40	0.99912
424	Carbosap	3	323.14	323	G	323.14	0.99991
427	Pasteur II	3	324.68	325	H	323.26	0.99955
426	Pasteur I	—	322.96	323	G	323.26	0.99955
428	Sterne	—	—	—	—	—	—
419	Nard	1	320.35	320	D	323.68	0.99825
420	Fra2	1	327.47	327	I	323.68	0.99825
421	F4	12	321.49	321	E	323.64	0.99838
425	Ferrara	12	316.75	317	A	322.73	1.00119

^a All examined samples have a local identification (ID) from a PostgreSQL database. The forensic codes and names, arbitrarily shortened, are reported in column 2. The genotype of pXO1- or pXO2-deficient strains (samples 426 and 428) were not included due to incomplete VNTR patterns. Samples were grouped according to the resulting subtype (column 6). The variability of each electrophoretic run (columns 4 and 7) was automatically corrected (column 5) with the help of a Microsoft Excel spreadsheet. Values reported in columns 4, 5, and 7 are the apparent lengths of fragments expressed in base pairs.

^b Overall mean, 323.11 (standard deviation, 0.34).

(sample 457) overlapped perfectly with Carbosap_{hex} (sample 424). These results were consistent with sequencing data (data not shown). As expected, the Pasteur II strain 74.12 used in the present study showed the two-plasmid pattern pXO1⁺/pXO2⁺, a finding consistent with the reference data (15, 21). More interestingly, when pXO2-A profile of Pasteur II (sample 427) was compared to Carbosap_{hex} (sample 424) a shift in the peaks (Fig. 2, group H) was revealed that was clearly due to a different A contents of VX2-3 poly(A). These data were confirmed by sequencing analysis (data not shown).

When the pXO2-A test was performed as nested PCR by using PCRs 24 and 28 sequentially, it became highly sensitive, with an increase by 10³ in the second round of reactions. Because this aspect was beyond the aims of our work, we did not go further with these sensitivity tests. As a rule, pXO2-A 28 was executed directly on the sample DNA without preamplification. Carbosap labeled in two different ways, PCR 28 (fam) and PCR 29 (hex), yielded perfectly overlapping peaks in the predicted range.

In order to confirm results in another range of molecular weights, the reverse primer 420-r of the above-mentioned sets was substituted with primer 464-r in a parallel set of PCRs (pXO2-A, PCR 27). The fluorescent fragments peaked just between the 200- and 245-kb size markers (data not shown).

Because no improvement of the resolution was obtained in this location, no further experiments were carried out with these alternative tests.

As expected, Stern vaccine (pXO1⁺/pXO2⁻) used as negative control for pXO2 plasmid tests showed no signal.

Figure 3 reports all of the genotyping results in a single graph. The START freeware programs turned out to be a very reliable tool for showing taxonomic relationships among strains. An unweighted pair group method with arithmetic means was easily applied starting from a data spreadsheet. It is generally not considered a good algorithm for construction of phylogenetic trees since it requires rates of evolution among different lineages to be approximately equal. Even if phylogenetic inferences could not be drawn from the clustering pattern seen with this method, it may prove useful as a quick guide for identifying similar isolates.

DISCUSSION

The experimental results were consistent with the “in silico” predictions, and the pXO2-A test was highly informative as a genetic marker. As recently reported (14), single-nucleotide repeats are extremely powerful markers for distinguishing among isolates where the predicted genetic diversity of the

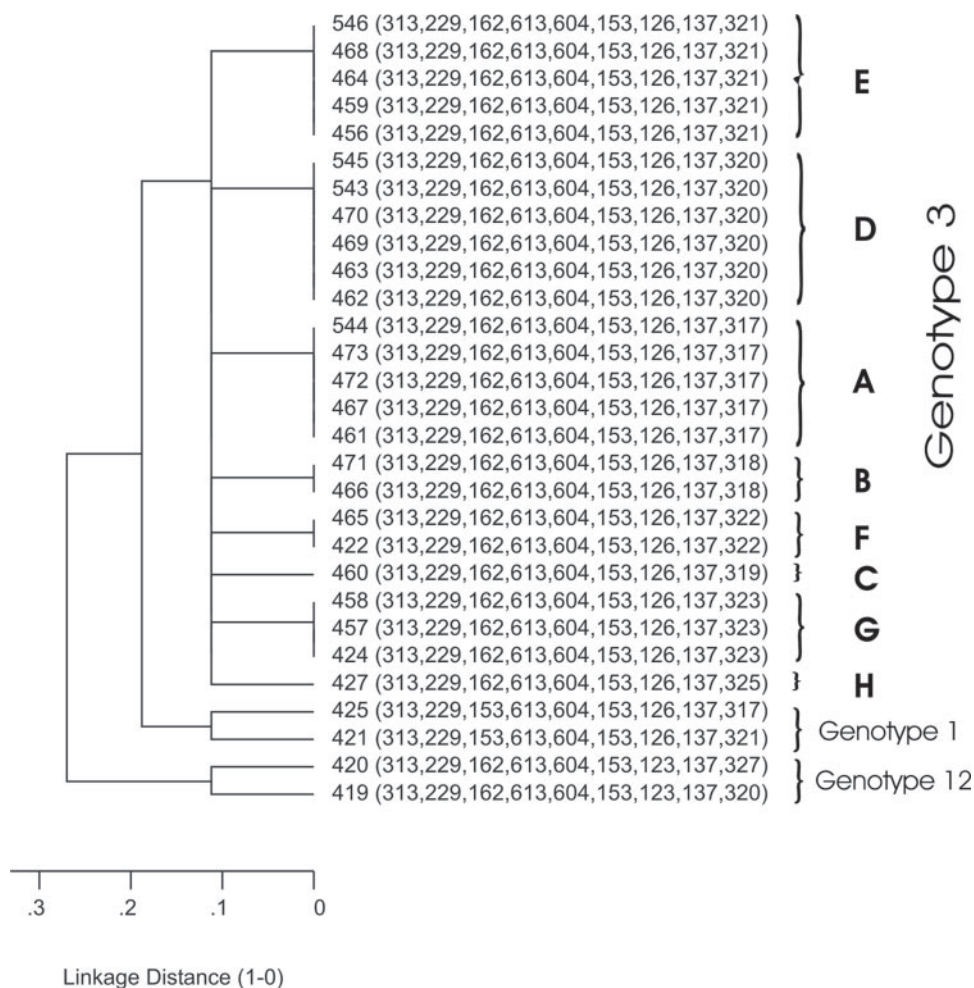


FIG. 3. Phylogenetic representation of 9-MLVA. Computed base pair lengths for all nine loci were reported in the START spreadsheet from which a UPGMA (unweighted pair-group method with arithmetic averages) tree was inferred. The 8-MLVA was central to determining three major phylogenetic patterns, corresponding to the genotypes 1, 12, and 3. The progressive hierarchical addition of the high-resolution pXO2-A assay results, maximizing the phylogenetic accuracy, subdivided the 23 isolates of genotype 3 into eight unique subtypes. Both genotypes 1 and 12 were divided into two subtypes. Allelic profiles are shown along with the isolate names. The pXO1- or pXO2-deficient strains were not included due to incomplete 8-MLVA patterns. The linkage distance attempts to measure the detected association between alleles at different loci (16).

isolates is extremely low. The pXO2-A test described here provides an accurate and rapid protocol that is particularly useful for distinguishing 91.3% of the genotype 3 (GT3) *B. anthracis* strains circulating in Italy from the live attenuated Carbosap vaccine. In contrast to sequencing, it does not require DNA purification, and the assay can be performed immediately after PCR. The four-color ABI chemistry enabled us to use more than one internal standard, hence reinforcing peak size computation. The limited number of GT3 samples tested in the present study is due to the fact that this genotype accounts for roughly 20% of wild isolates. In fact, the most frequent genotype in Italy is genotype 1, in contrast to France (8) and North America, where GT3 predominates.

The confirmation of a two-plasmid pattern in the attenuated *B. anthracis* strain Pasteur type II strain 74.12, such as Carbosap, is consistent with their similar biological properties related to attenuation characteristics and residual pathogenicity. It could be hypothesized that plasmid-encoded and chromosomal genes act synergistically in the global virulence of *B.*

anthracis. Therefore, mechanisms still unknown could play a role in the attenuation of the *B. anthracis*.

These data are very interesting because they further underline the importance of being able to distinguish between Carbosap and Pasteur strain type II. In fact, OIE tests are not able to adequately identify vaccine strains closely related to Carbosap and Pasteur II strain 74.12. This method may therefore complete the diagnostic techniques required by OIE (18) for test confirmation of the virulence of strains isolated from anthrax outbreaks.

Although the method may be less useful in countries where the Sterne vaccine is widely used, the pXO2-A marker may be adopted everywhere as an alternative to the identification test recommended by the European Pharmacopoeia (6), since it is more informative, less expensive, and faster.

In conclusion, the molecular method presented here could follow the 8-MLVA as a second step of a new hierarchical standard protocol intended to differentiate Carbosap live vaccine from pathogen strains of *B. anthracis* belonging to geno-

type 3. Future efforts will be necessary to find other loci that enable us to also differentiate subtype G samples, which have the same pXO2-A profile as CarboSap, for more accurate forensic and epidemiological analyses of natural anthrax cases.

ACKNOWLEDGMENTS

We thank Paolo Pastori for excellent technical assistance and contribution in the computational part of this study.

This study was partly supported by the project "Potabilizzazione Delle Acque e Rischi Sanitari Emergenti (PARSE): Marcatori genetici di microrganismi patogeni e diagnostica PCR" of the Italian Ministry of Health (ISS protocol N. 3 ANF).

REFERENCES

1. Adone, R., P. Pasquali, G. La Rosa, C. Marianelli, M. Muscillo, A. Fasanella, M. Francia, and F. Ciuchini. 2002. Sequence analysis of the genes encoding for the major virulence factors of *Bacillus anthracis* vaccine strain CarboSap. *J. Appl. Microbiol.* **93**:117–121.
2. Anonymous. 2001. Update: investigation of bioterrorism-related inhalational anthrax—Connecticut, 2001. *Morb. Mortal. Wkly. Rep.* **50**:1049–1051.
3. Atlas, R. M. 2002. Bioterrorism: from threat to reality. *Annu. Rev. Microbiol.* **56**:167–185.
4. Bales, M. E., A. L. Dannenberg, P. S. Brachman, A. F. Kaufmann, P. C. Klatsky, and D. A. Ashford. 2002. Epidemiologic response to anthrax outbreaks: field investigations, 1950–2001. *Emerg. Infect. Dis.* **8**:1163–1174.
5. Cataldi, A., M. Mock, and L. Bentancor. 2000. Characterization of *Bacillus anthracis* strains used for vaccination. *J. Appl. Microbiol.* **88**:648–654.
6. EDQM. 2002. Anthrax spore vaccine (live) for veterinary use, p. 2229–2290. *In* European Pharmacopeia, 4th ed. European Directorate for the Quality of Medicine, Strasbourg, France.
7. Fasanella, A., S. Losito, T. Trotta, R. Adone, S. Massa, F. Ciuchini, and D. Chiocco. 2001. Detection of anthrax vaccine virulence factors by polymerase chain reaction. *Vaccine* **19**:4214–4218.
8. Fouet, A. S., K. L. Smith, C. Keys, J. Vaissaire, C. Le Doujet, M. Levy, M. Mock, and P. Keim. 2002. Diversity among French *Bacillus anthracis* isolates. *J. Clin. Microbiol.* **40**:4732–4734.
9. Greene, C. M., J. Reefhuis, C. Tan, A. E. Fiore, S. Goldstein, M. J. Beach, S. C. Redd, D. Valiante, G. Burr, J. Buehler, R. W. Pinner, E. Bresnitz, and B. P. Bell. 2002. Epidemiologic investigations of bioterrorism-related anthrax, New Jersey, 2001. *Emerg. Infect. Dis.* **8**:1048–1055.
10. Griffith, K. S., P. Mead, G. L. Armstrong, J. Painter, K. A. Kelley, A. R. Hoffmaster, D. Mayo, D. Barden, R. Ridzon, U. Parashar, E. H. Teshale, J. Williams, S. Noviello, J. F. Perz, E. E. Mast, D. L. Swerdlow, and J. L. Hadler. 2003. Bioterrorism-related inhalational anthrax in an elderly woman, Connecticut, 2001. *Emerg. Infect. Dis.* **9**:681–688.
11. Jolley, K. A., E. J. Feil, M. S. Chan, and M. C. J. Maiden. 2001. Sequence type analysis and recombinational tests (START). *Bioinformatics* **17**:1230–1231.
12. Keim, P., A. Kalif, J. Schupp, K. Hill, S. E. Travis, K. Richmond, D. M. Adair, M. Hugh-Jones, C. R. Kuske, and P. Jackson. 1997. Molecular evolution and diversity in *Bacillus anthracis* as detected by amplified fragment length polymorphism markers. *J. Bacteriol.* **179**:818–824.
13. Keim, P., L. B. Price, A. M. Klevytska, K. L. Smith, J. M. Schupp, R. Okinaka, P. J. Jackson, and M. E. Hugh-Jones. 2000. Multiple-locus variable-number tandem repeat analysis reveals genetic relationships within *Bacillus anthracis*. *J. Bacteriol.* **182**:2928–2936.
14. Keim, P., M. N. Van Ert, T. Pearson, A. J. Vogler, L. Y. Huynh, and D. M. Wagner. 2004. Anthrax molecular epidemiology and forensics: using the appropriate marker for different evolutionary scales. *Infect. Genet. Evol.* **4**:205–213.
15. Makino, S. I., H. I. Cheun, M. Watarai, I. Uchida, and K. Takeshi. 2001. Detection of anthrax spores from the air by real-time PCR. *Lett.* **33**:237–240.
16. Maynard-Smith, J., N. H. Smith, M. O'Rourke, and B. G. Spratt. 1993. How clonal are bacteria? *Proc. Natl. Acad. Sci. USA* **90**:4384–4388.
17. Oggioni, M. R., F. Meacci, A. Carattoli, A. Ciervo, G. Orru, A. Cassone, and G. Pozzi. 2002. Protocol for real-time PCR identification of anthrax spores from nasal swabs after broth enrichment. *J. Clin. Microbiol.* **40**:3956–3963.
18. Organization International Epizooties. 2004. Manual of diagnostic tests and vaccines for terrestrial animals, p. 1–20. OIE, Paris, France.
19. Read, T. D., S. N. Peterson, N. Tourasse, L. W. Baillie, I. T. Paulsen, K. E. Nelson, H. Tettelin, D. E. Fouts, J. A. Eisen, S. R. Gill, E. K. Holtzapple, O. A. Okstad, E. Helgason, J. Rilstone, M. Wu, J. F. Kolonay, M. J. Beanan, R. J. Dodson, L. M. Brinkac, M. Gwinn, R. T. DeBoy, R. Madpu, S. C. Daugherty, A. S. Durkin, D. H. Haft, W. C. Nelson, J. D. Peterson, M. Pop, H. M. Khouri, D. Radune, J. L. Benton, Y. Mahamoud, L. X. Jiang, I. R. Hance, J. F. Weidman, K. J. Berry, R. D. Plaut, A. M. Wolf, K. L. Watkins, W. C. Nierman, A. Hazen, R. Cline, C. Redmond, J. E. Thwaite, O. White, S. L. Salzberg, B. Thomason, A. M. Friedlander, T. M. Koehler, P. C. Hanna, A. B. Kolsto, and C. M. Fraser. 2003. The genome sequence of *Bacillus anthracis* Ames and comparison to closely related bacteria. *Nature* **423**:81–86.
20. Read, T. D., S. L. Salzberg, M. Pop, M. Shumway, L. Umayam, L. X. Jiang, E. Holtzapple, J. D. Busch, K. L. Smith, J. M. Schupp, D. Solomon, P. Keim, and C. M. Fraser. 2002. Comparative genome sequencing for discovery of novel polymorphisms in *Bacillus anthracis*. *Science* **296**:2028–2033.
21. Uchida, I., T. Sekizaki, K. Hashimoto, and N. Terakado. 1985. Association of the encapsulation of *Bacillus anthracis* with a 60-megadalton plasmid. *J. Gen. Microbiol.* **131**:363–367.